MAPPING EQUATORIAL IONOSPHERIC PROFILES OVER PENINSULAR MALAYSIA USING GPS TOMOGRAPHY

SITI SYUKRIAH BINTI KHAMDAN

A thesis submitted in fulfilment of the
requirements for the award of the degree of
Master of Philosophy

Faculty of Built Environment and Surveying
Universiti Teknologi Malaysia

NOVEMBER 2018

DEDICATION

Dedicated to My Loving Family & My In-Law

Mr Khamdan Ali

Mdm Fatimah Nurhaizawati Muhi

Siti Nurfadhillah Khamdan

Mohd. Aminuddin Khamdan

Mr Ahmad Nasaruddin Ishaudin

Mdm Norlida Mohd Nor

Nur Alya Ferdaus

Ahmad Haziq Ferdaus

Ahmad Rizqin Ferdaus

Nur Arina Ferdaus

Thank you for the Doa', encouragement, supports and inspiration.

To My Beloved One

Ahmad Nashriq Ferdaus

Thank you for your supports and understanding.

Lastly, To My Supervisors

PM Dr Tajul Ariffin Musa & Dr Suhaila M. Buhari

Thank you for your guidance, opportunity, knowledges and experiences.

ACKNOWLEDGEMENT

Alhamdulillah, first and foremost, thanks to Allah S.W.T who has provided guidance, opportunity and knowledge to complete this thesis.

In particular, I wish to express my gratitude to both of my supervisors, *Assoc Prof Dr Tajul Ariffin Musa* and *Dr Suhaila M Buhari*, for their encouragement, guidance, critics and supervisions whilst undertaking this study. Thank you also to *Dr Dudy Darmawan Wijaya* for his guidance and knowledge to improve and guidance to complete this study. Without their support, guidance and critics, this thesis would not have been the same as presented here.

Special appreciation to *Department of Survey and Mapping Malaysia* (DSMM), *IGS analysis centre, IRI and NeQuick committee* for providing the relevant information and data. Special thanks also to *NICT, Japan* and *LAPAN, Indonesia* for providing the ionosonde data measurement. Thank you also to *Dr Mariyam* from UTHM for assistance in interpretation of ionosonde data, *ANGKASA Malaysia* and *UTM* for providing funding to support this study.

To all my *Geomatics Innovation Research Group (GnG) members*, especially to Abang Leong, Kak Suriati, Yusuf, Kak Anim, Adzlan, Amir Hamzah, Amirul, Suhaila, Suraya, Syazwan, Nini and Jehan, thank you very much for your advice and helps during my study. Their views and tips are useful indeed. Lastly, sincere appreciation extends to *ISELION 2015, IRI 2017 and IceSSat2018* participants and committees for sharing their knowledge, encouragement and inspiration that guide me to continue focus in this study.

ABSTRACT

The ionospheric conditions over Malaysia are profoundly critical not only due to its location that is near to the equator but also due to the high solar activity that occurred during the 11-years solar cycle. The two-dimensional (2D) single thin layer model (SLM) has been widely used to monitor and model the ionosphere. However, this model only focuses on the height of the maximum densities of the electron, which lies within 300 kilometre (km) to 450 km above the Earth and therefore neglects the information of bottom and topside of the ionosphere. Hence, a three-dimensional (3D) ionospheric structure is proposed to address these limitations. The aim of this study is to model the electron density profile over Peninsular Malaysia using Global Positioning System (GPS) ionospheric tomography method. In doing so, the Malaysian Real-time Kinematic Network (MyRTKnet) over Malaysia was utilized to derive the total electron content (TEC) maps. It was found that the variations of the TEC increase with decreasing of latitude and longitude, and gradually change from East to West direction. The GPS-derived TEC from the years 2009 to 2014 shows that the maximum yearly mean TEC over Malaysia is up to 58 TEC unit (TECU), recorded during the year 2014 which was associated with high sunspot numbers. The maximum yearly mean and the minimum peak of diurnal variations occur at 08 universal time (UT) and 21UT respectively. Next, the receiver code bias (DCB_r) was estimated for MyRTKnet stations using the adopted algorithm from IONOLAB-BIAS. For assessment purpose, this method shows a good estimation of DCB_r with the International Global Navigation Satellite System (GNSS) Service (IGS) analysis centre compared to with Bernese software. Then, the GPS ionospheric tomography module was developed to reconstruct the electron density profile over Peninsular Malaysia. The results were validated with the nearest ionosonde station and the ionospheric global models such as the International Reference Ionosphere (IRI) model and NeQuick model. It was found that the differences between GPS ionospheric tomography with the models are small during the daytime but large at night-time. It was also found that, the GPS ionospheric tomography appears to be more agreeable with the IRI model than with NeQuick model. For the validation of the NmF2 parameters with the IRI model and ionosonde measurements, the GPS ionospheric tomography is more agreeable with the ionosonde than with the IRI model. The results also show that the GPS ionospheric tomography is capable to show the vertical ionospheric profile over the study area during quiet ionospheric conditions and its irregularities during disturbed conditions of the ionosphere. Overall, it was found that the GPS ionospheric tomography method is suitable for examining and monitoring the ionospheric variations and irregularities in support of the space weather studies in Peninsular Malaysia.

ABSTRAK

Keadaan ionosfera di Malaysia amat kriktikal bukan hanya kerana lokasinya yang berhampiran dengan garisan khatulistiwa, tetapi juga dipengaruhi oleh aktiviti suria yang berlaku ketika 11 tahun kitaran suria. Model dua dimensi (2D) lapisan tipis tunggal (SLM) telah digunakan secara meluas untuk pemantauan dan pemodelan ionosfera. Walau bagaimanapun, model ini hanya tertumpu kepada ketinggian maksimum kepadatan elektron, yang terletak dalam jarak 300 kilometer (km) hingga 450 km di atas Bumi dan oleh itu ia mengabaikan informasi bahagian bawah dan atas ionosfera. Oleh yang demikian, struktur ionosfera tiga dimensi (3D) telah dicadangkan untuk mengatasi kekangan ini. Tujuan kajian ini adalah untuk memodelkan profil kepadatan elektron di Semenanjung Malaysia menggunakan kaedah tomografi ionosfera Sistem Penentududukan Sejagat (GPS). Oleh yang demikian, Jaringan GPS Kinematik Masa Hakiki Malaysia (MyRTKnet) telah digunakan untuk menerbitkan peta jumlah kandungan elektron (TEC). Didapati bahawa variasi TEC meningkat dengan penurunan latitud dan longitud, dan secara beransur berubah dari arah Timur ke Barat. TEC daripada GPS diperoleh, dari tahun 2009 hingga 2014 menunjukkan bahawa purata maksimum tahunan TEC ke atas Malaysia adalah 58 unit TEC (TECU), yang direkodkan pada tahun 2014 selari dengan nombor tompok matahari yang tinggi. Purata tahunan maksimum dan minimum bagi puncak variasi harian masing-masing berlaku pada jam 08 dan 21 waktu piawai (UT). Seterusnya, kecenderungan kod penerima (DCB_r) telah dianggarkan bagi stesen MyRTKnet dengan menggunakan algoritma yang diadaptasi daripada IONOLAB-BIAS. Untuk tujuan penilaian, kaedah ini menunjukkan anggaran DCB_r yang baik dengan pusat analisis Perkhidmatan Sistem Satelit Navigasi Sejagat (GNSS) Antarabangsa (IGS) berbanding dengan perisian Bernese. Kemudian, modul tomografi ionosfera GPS dibangunkan untuk membina semula profil ketumpatan elektron di Semenanjung Malaysia. Hasilnya telah disahkan dengan stesen ionosonde yang terdekat dan model global ionosfera seperti model Rujukan Ionosfera Antarabangsa (IRI) dan model *NeQuick*. Didapati bahawa perbezaan antara tomografi ionosfera GPS dan model adalah kecil pada waktu siang dan besar pada waktu malam. Selain itu, didapati juga tomografi ionosfera GPS kelihatan lebih sesuai dengan model IRI berbanding dengan model NeQuick. Bagi tujuan penilaian parameter NmF2 dengan model IRI dan ukuran ionosonde, tomografi ionosfera GPS menunjukkan ianya lebih sepadan dengan ukuran ionosonde berbanding dengan model IRI. Hasil kajian juga menunjukkan bahawa tomografi ionosfera GPS mampu menunjukkan profil ionosfera tegak bagi kawasan kajian ketika kodisi ionosfera yang senyap dan gangguan ketika kondisi ionosfera yang terganggu. Secara keseluruhannya, didapati bahawa kaedah ionosfera GPS tomografi sesuai digunakan di Semenanjung Malaysia bagi tujuan kajian dan pemantauan variasi ionosfera bagi membantu kajian cuaca angkasa di Semenanjung Malaysia.

TABLE OF CONTENTS

LIST OF TABLES

LIST OF FIGURES

FIGURE NO. TITLE PAGE

LIST OF ABBREVIATIONS

2D	-	Two-dimensional
3D	-	Three-dimensional
ART	-	Algebraic Reconstruction Technique
CODE	-	Centre for Orbit Determination in Europe
CORS	-	Continuously operating reference station
COSPAR	-	Committee on Space Research
DCB	-	Differential code bias
DCB_r	-	Receiver code bias
DCB^s	-	Satellite code bias
DSMM	-	Department of Survey and Mapping Malaysia
EEJ	-	Equatorial electrojet
EIA	-	Equatorial ionization anomaly
EOP	-	Earth Orientation Parameter
EPB	-	Equatorial plasma bubble
ESA	-	European Space Agency
ESF	-	Equatorial spread-F
EUV	-	Extreme ultraviolet
GEONET	-	GPS Earth Observation Network
GIM	-	Global Ionosphere Maps
GIRO	-	Global Ionosphere Radar Observatory
GNSS	-	Global Navigation Satellite System
GPS	-	Global Positioning System
HF	-	High-frequency
hmF_2	-	Height of the peak of electron density of F_2 layer
ICTP	-	T/ICT4D Laboratory of the Abdus Salam International Centre for Theoretical Physics
IGS	-	International GNSS Service
IONEX	-	ionosphere map exchange format
IPP	-	Ionospheric pierce points
IRI	-	International Reference Ionosphere

ISIS	-	International Satellite for Ionosphere
JPL	-	Jet Propulsion Laboratory
KGN	-	Korean GPS Network
km	-	Kilometre
LAPAN	-	National Institute of Aeronautics and Space, Indonesia
LSE	-	Least square estimation
MARS	-	Multivariate Adaptive Regression Splines
MART	-	Multiplicative Algebraic Reconstruction Technique
MF	-	Mapping function
ML	-	Maximum Likelihood
MSTID	-	Medium-scale travelling ionospheric disturbances
MyRTKnet	-	Malaysian Real-time Kinematic Network
NASA	-	National Aeronautics and Space Administration
NBOS	-	National Blue Ocean Strategy
NICT	-	National Institute of Information and Communication Technology
NmF_2	-	Electron density peak of F_2 layer
NOAA	-	National Oceanic and Atmospheric Administration
NRC-net	-	National R&D GPS CORS
ns	-	Nanosecond
PLM	-	Path length matrix
ROT	-	Rate of TEC change
ROTI	-	Rate of changes TEC index
ROT_{Ne}	-	Rate of change electron density
RTI	-	Rayleigh-Taylor instability
RTK	-	Real-time kinematic
SEALION	-	Southeast Asia Low-Latitude Ionospheric Network
SIRT	-	Simultaneous Iterative Algebraic Reconstruction Technique
SLM	-	Single layer model
SP3	-	IGS precise final orbit
SSN	-	Sunspot number
STEC	-	Slant total electron content
SuGAr	-	Sumatran GPS Array

SVD	-	Singular value decomposition
SWPC	-	Space Weather Prediction Centre
TEC	-	Total electron content
TECU	-	Total electron content unit
UPC	-	Polytechnic University of Catalonia
URSI	-	International Union of Radio Science
UT	-	Universal time
VTEC	-	Vertical total electron content
WDC	-	World Data Centre for Geomagnetism
ZD	-	Zero difference

LIST OF SYMBOLS

±	-	Plus-minus sign
°	-	Degree
B	-	Magnetic field
$\boldsymbol{r}, \boldsymbol{s}$	-	Receiver and satellite
$\boldsymbol{N_e}$	-	Electron density
$\boldsymbol{l}$	-	Signal ray path
el/m^2	-	Electron per meter square
f_1, f_2, f_5	-	GPS frequencies
MHz	-	Megahertz
$\boldsymbol{\phi_1}, \boldsymbol{\phi_2}$	-	Carrier phase measurement
$\boldsymbol{P_1}, \boldsymbol{P_2}$	-	Pseudorange measurement
$\boldsymbol{\rho}$	-	Geometric range from satellite to receiver
$\boldsymbol{c}$	-	Speed of light
$\boldsymbol{dt^s}, \boldsymbol{dt_r}$	-	Satellite and receiver clock delay
$\boldsymbol{d_{ion}}$	-	Ionospheric delay
$\boldsymbol{d_{trop}}$	-	Tropospheric delay
$\boldsymbol{d_{mp}}$	-	Multipath
$\boldsymbol{\lambda}$	-	Wavelength
$\boldsymbol{N}$	-	Carrier phase integer ambiguity (Chapter 2)
$\boldsymbol{\varepsilon}$	-	Signal noise
$\boldsymbol{\phi_4}, \boldsymbol{P_4}$	-	Linear combination geometry-free
N, E	-	North, East
R	-	Earth radius
h	-	Ionospheric shell height
n_{max}	-	Maximum degree of the spherical harmonic expansion
$\tilde{P}_{nm} = \Lambda(n,m)P_{nm}$	-	The normalized Legendre functions
β	-	Geocentric latitude of the IPP

a_{nm}, b_{nm}	-	The unknown global/regional ionosphere model coefficients
s	-	Sun-fixed longitude of the IPP
%	-	Percent
Y	-	Vector of observed STEC data
A	-	The geometry matric that describe the relationship between line of sight of TEC or also known as the path length matrix (PLM) and electron density
x	-	The unknown vector (electron density)
E	-	Errors during the approximation in calculation
m	-	Number of rays
N	-	Number of voxels (Chapter 4)
x_{kk}	-	The electron density values at kk voxel
d_{ij}	-	Length of ray path travelled through the voxel kk
x_j^{k+1}	-	The modified electron densities in design voxel
x_j^k	-	The *j*th member of a vector of N unknowns at the *k*th iteration
$\langle A^i, x^k \rangle$	-	Back-projection of the *i*th observation after the *k*th iteration
y_i	-	The ith row of the matrix *Y*
A^i	-	The *i*th row of the matrix A
λ	-	The relaxation parameter (Chapter 4)
F_c	-	Critical frequency
N_e	-	Electron density in m^3
nT	-	Nanotesla

LIST OF APPENDICES

CHAPTER 1

INTRODUCTION

1.1 Background of Study

1.1.1 Overview of Ionosphere

The ionosphere is a layer that lies on the upper region of atmosphere approximately within 70 kilometre (km) to 1000 km above the Earth's surface. It consists of free electrons and ions of thermal energy that exist under the control of gravity and magnetic field of the Earth (Zolesi and Cander, 2014). The ionization in the ionosphere layer often become turbulent and develop electron densities irregularities (Ray *et al.*, 2006). The ionosphere layer can be categorized into several layers which are D-layer, E-layer and F-layer in ascending height order. This characterization is classified based on its free, neutral and charged particles that vary by time of day.

Based on Figure 1.1, the D-layer lies at the bottom part of the ionosphere approximately between 70 km to 90 km that vary by sunlight. The rate of ionization of D-layer is due to the charged particles in the magnetosphere which is mainly depends on the geomagnetic latitudes and geomagnetic activities (Tan *et al.*, 2017). According to Tan *et al.* (2015), since the recombination process are too fast over this layer, it makes the electron densities very low, particularly during the night-time. The D-layer absorbs the high frequency radio waves and reflect the low frequency waves.

The E-layer lies above the D-layer approximately between 90 km to 160 km. The ionization in this layer is caused by the ultraviolet and x-rays during the day, and cosmic rails and meteor during the night-time. This layer remains weekly ionized during the night-time, but it did not completely disappear. The E-layer also exhibits the Chapman model behaviour of daily maximum at local noon, seasonal maximum in

summer and solar cycle dependence (Zolesi and Cander, 2014). The Sproadic E-layer or known as Es-layer also occurs at the E-layer. This layer varies between 80 km to 120 km and appears at any time of day with a preference for the late morning and early evening.

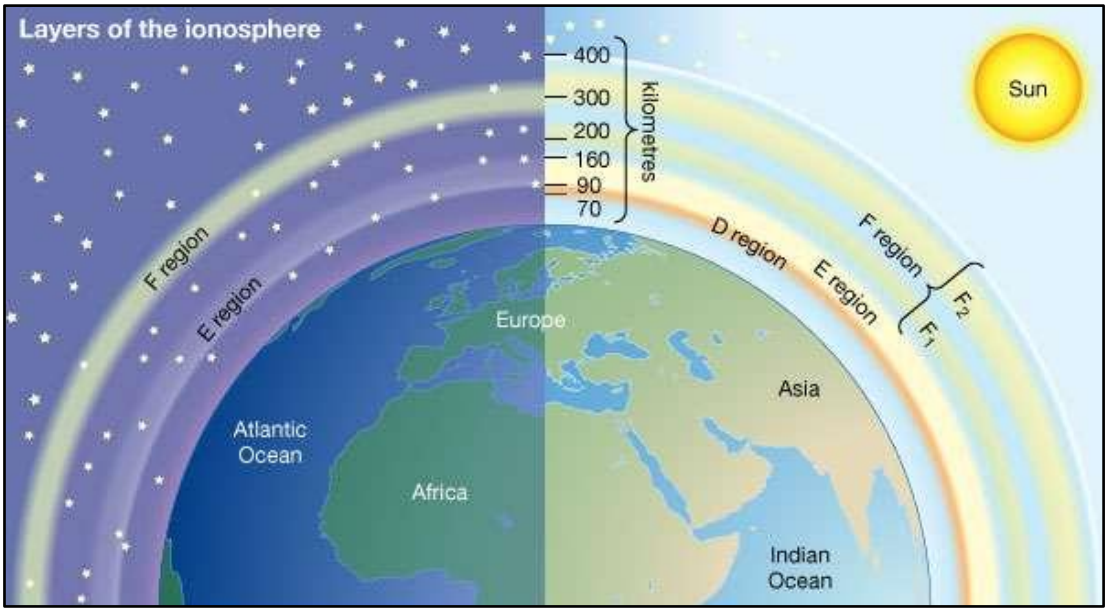

Figure 1.1 The profile of ionosphere during daytime and night-time (Source: Encyclopedia Britannica, 2017).

The major layer of the ionosphere known as the F-layer lies above 150 km. It can be divided into two minor layers, F_1-layer (within 150 km to 200 km) and F_2-layer (within 200 km to 1000 km), due to the solar radiation. After sunset, both of this layer always merge and reshape to F-region. The F_1-layer is ionized by extreme ultraviolet (EUV) solar radiation and always disappear during the night-time. Meanwhile, F_2-layer presents 24 hours a day under all solar terrestrial conditions. This layer has been main focus by most of the ionospheric studies due to its maximal densities of electron and its effects towards communication and navigation system (Hoffman-Wellenhof *et al.*, 2007).

1.1.2 The Ionospheric Conditions over the Equatorial Region

The Earth are divided into three major geographical regions of ionosphere which are equatorial or low-latitude (±20° of geomagnetic equator), middle-latitude

(from ±20° to ±60° of geomagnetic equator) and high latitude or aurora region. Figure 1.2 shows the classification of the ionosphere's geographical regions

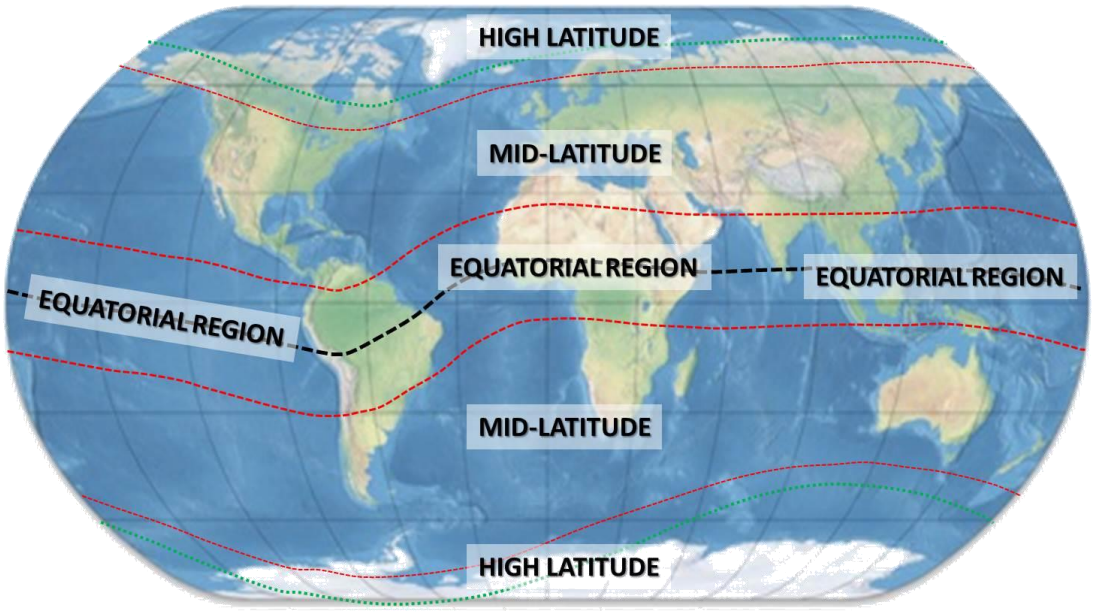

Figure 1.2 The geographical region of the ionosphere (Modified from Wikipedia, 2018).

The equatorial region is well known with its unique conditions of the ionosphere due to the magnetic field (*B*) nearly parallel to the Earth's surface (Ray *et al.*, 2006). This region has been reported to have numbers of ionospheric irregularities, such as equatorial electrojet (EEJ), equatorial plasma bubbles (EPB), equatorial spread-F (ESF), equatorial ionization anomaly (EIA) and others. It has been reported that the global maximum of electron densities, time delay, scintillation and the large gradient in the spatial distribution of the electron densities are contributed by the occurrence of the ionospheric irregularities over equator (Abdu, 2005; Aggarwal, 2011; Leong, 2013; Oryema *et al.*, 2016).

1.1.3 Global Positioning System for Ionospheric Studies

Past two decades, the Global Positioning System (GPS) has been widely used in ionospheric studies and monitoring. Since the GPS has a dense continuously operating reference station (CORS) network over the world, it has been a powerful tool for ionospheric estimation and monitoring for local and global scale. Unlike GPS,

the other instruments such as ionosonde, magnetometer, airglow and scatter radar have high maintenance cost and dysfunctionality which may lead to the large data gap.

By using GPS for ionospheric studies, the estimation of ionosphere usually presented in terms of total electron content (TEC) in two-dimensional (2D) (in terms of latitude-longitude), where the mapping function single layer model (SLM), is used. The SLM converted the line of sight TEC to the vertical TEC by assuming the ionosphere is compressed onto a thin shell at the ionospheric height within 300 km to 450 km. At this height, the ionosphere is expected to have maximum numbers of electron densities and gives the largest effects on the GPS signals (Ya'acob *et al.*, 2010; Musa *et al.*, 2012; Leong *et al.*, 2015).

However, the SLM mapping function neglect the vertical information of the ionosphere and limits the capability of GPS to map the vertical structure of ionosphere. Therefore, the three-dimensional (3D) models of electron density (in terms of latitude-longitude-height) have been developed to obtain the vertical information of ionosphere using the tomography method.

In this study, a 3D ionospheric electron density profile is reconstructed by using the tomography method. The reconstruction covered the Peninsular Malaysia area where a dense of GPS CORS network, i.e., the Malaysian Real-Time Kinematic Network (MyRTKnet), has been used. The tomography module has been developed and the assessment of the module has been carried out with global models and any in-situ measurement that are available. This will act as a validation step to prove the capability of the tomography method to reconstruct the ionospheric distribution over the study area. In addition, some case studies have been selected to test the capability of the module in detection the ionospheric phenomenon over the study area.

1.2 Problem Statement

There are five (5) main problems that need to be solved in this study.

i. Ionospheric Global Model

The existing global model such as International Reference Ionosphere (IRI) model and NeQuick model are widely used in ionospheric studies. Both models are based on the worldwide data measurements which best describe the global conditions of ionosphere. In Malaysia, there is no in-situ measurement that have been reported which contribute to the development of both models. Hence, the conditions of ionosphere from the models are only based on the interpolation data and it is less accurate in describing the local conditions of ionosphere.

ii. Unique Ionospheric Conditions over Equatorial Region

The equatorial region has a unique condition of ionosphere as it has many occurrences of ionospheric irregularities. This region is well-known as the highest values of the electron content and large gradient in the spatial distribution of the electron density. Malaysia is located near geomagnetic equator and its ionospheric conditions are profoundly severe. The conditions of the ionosphere over this region are also highly affected by the visibility of the sunspots, time of day, time of year and level of solar activity (Leong *et al.*, 2009). Therefore, it is important to understand the ionospheric conditions over Malaysian region.

iii. Classical Technique Measurement

Most of the ionospheric studies in Malaysia are based on the classical techniques, such as ionosonde and magnetometer. These instruments have a limited spatial and temporal coverage as well as high maintenance cost, which usually lead to large data gaps, hence limits the ability for continuous ionospheric studies. In contrast, the existing dense GPS CORS network over Peninsular Malaysia, MyRTKnet, could be utilized to estimate the ionospheric parameters and consequently give the opportunity to model the ionospheric profile over this region

iv. Limitation of Single Layer Model (SLM)

Most of the ionospheric studies focus on the F-layer since this layer emits numbers of ionospheric phenomenon. By adopting SLM mapping function, the GPS measurement estimated the ionosphere at the altitude of the maximum densities of the electron approximately within 350 km to 450 km. This would limit the ability to obtain the variation of the ionosphere over the D-layer and E-layer. Hence, the ionospheric profile will remain unknown and it is difficult to obtain the electron density profile.

v. Reconstruction Inversion Model

The GPS measurements only provide slant TEC (STEC) along the signal path of satellites to receivers. Since the electron density profile of ionosphere is important in ionospheric studies, the STEC need to be inverted to reconstruct the electron density profile of the ionosphere. Hence, an appropriate inversion model is required. In addition, the reconstruction design needs to consider a large amount of STEC data from GPS CORS network over the Peninsular Malaysia.

1.3 Aim and Objective

The aim of this study is to model the electron density profile over Peninsular Malaysia.

To achieve this aim, there are three (3) specific objectives need to be accomplished:

i. To monitor the trend of ionosphere by using ionospheric TEC maps.

The GPS observation data for six (6) years over Malaysian region have been used to generate the TEC maps. Then, the trend of ionosphere based on the

maps has been analysed by taking account on its diurnal, spatial and seasonal variation.

ii. To reconstruct the electron densities profile using GPS tomography

The ionospheric GPS tomography module has been developed for reconstruction of electron densities profile. The reconstruction over the study area has been conducted to determine the suitability of the module in estimation of the electron density profile.

iii. To validate the assessment from (ii) by using ionosonde and global model

Two global models, IRI model and NeQuick model, and ionosonde measurement have been used to validate the reconstruction of the electron density profile from GPS tomography method.

1.4 Scope and Limitation

This study had defined the scope and limitation in reconstruction of electron density profile as follows:

i. A dense GPS CORS network in Malaysia, MyRTKnet, that managed by Department of Survey and Mapping Malaysia (DSMM) has been used for TEC estimation and reconstruction of electron density profile over the study area. Sumatran GPS Array (SuGAr) network has been used for the reconstruction of electron density profile with purposed to validate with ionosonde measurements at Sumatera Indonesia.

ii. There are numbers of available software from open source, commercial and scientific software that can be used for TEC estimation. In this study, the high-scientific software, Bernese software version 5.0 has been utilized to estimate the TEC. This software has a capability to handle high precision processing for TEC estimation. Meanwhile, Matlab software has been used for development of the GPS ionospheric

tomography module as well as for visualization of TEC maps and 3D electron density profile.

iii. The IRI model is managed by Committee on Space Research (COSPAR) and the International Union of Radio Science (URSI). Meanwhile, the NeQuick model has been developed by T/ICT4D Laboratory of the Abdus Salam International Centre for Theoretical Physics (ICTP). The nearest ionosonde station, located at Kototabang, Indonesia, is part of Southeast Asia Low-Latitude Ionospheric Network (SEALION) that is managed by the National Institute of Information and Communication Technology (NICT), Japan. In this study, the IRI model has been used as a background model/initial value for reconstruction of electron density profile. Kototabang ionosonde data act as a true value for comparison between IRI model, NeQuick model and reconstruction from tomography module.

iv. The GPS ionospheric tomography has been reconstructed over the Peninsular Malaysia only. This is due to no GPS CORS stations over the South China Sea and thus interpolation while reconstructed the electron density profile might be wrong. Other than that, the GPS CORS networks over Peninsular Malaysia are denser compared to Sabah and Sarawak.

1.5 Significance of Study

The significance of this study are as follows:

1. This study proposed a technique/method for reconstruction of electron densities profile over Peninsular Malaysia. This is due to the sparse network of the MyRTKnet stations over the Sabah and Sarawak. Since there is no GPS CORS over the South China Sea, the reconstruction of the GPS ionospheric tomography based on the interpolation might be wrong.

2. The tomography module using GPS measurements can be used to augment the classical technique such as ionosonde that has a limited spatial and temporal coverage as high in maintenance cost.

3. The reconstruction of GPS ionospheric tomography in this study best describes the local conditions of the ionosphere compared to the IRI model and NeQuick model, where both only best describe the global conditions of ionosphere.

4. The GPS ionospheric tomography capable to reconstruct the electron density profile, and can support in aviation, space weather studies, satellite communication and precise GPS positioning. For example, the reconstruction of the GPS ionospheric tomography can be applied for the real-time kinematic (RTK) application and high precision processing (post-process) to reduce the ionospheric delay that exists in the GPS measurements.

5. This study supports the developments in fundamental aspect on space weather studies and modelling the impact of the equatorial ionosphere in Malaysia that aligned with the National Space Policy 2023.

1.6 Research Methodology

The research methodology and workflow can be divided into five (5) main phases.

PHASE I: Research Planning and Study Area

1. In this phase, the research flow has been planned as shown in Figure 1.3.

2. Critical literature for this research has been continued together with the planning.

3. The research methodology has been designed based on literature to support the modelling of the electron densities profile over study area.

In this phase, the voxel size for GPS tomography was designed and proposed based on the study area.

PHASE II: Data Acquisition

1. GPS Measurement Data

In this study, two dense GPS CORS network, MyRTKnet and SuGAr network has been used to reconstruct the electron density profile over the study area.

Global Ionospheric Model

The global ionospheric models, IRI model and NeQuick model have been retrieved for validation of the reconstruction of GPS ionospheric tomography. The IRI model also used as a background model during the reconstruction. The IRI data have been retrieved from IRI website (http://irimodel.org/) while the NeQuick has been retrieved from the NeQuick 2 Web Model website (https://t-ict4d.ictp.it/nequick2/nequick-2-web-model).

Ionosonde Data

The ionosonde data from Kototabang, Indonesia also used to validate the reconstruction of electron density profile from GPS ionospheric tomography. The data have been retrieved from the NICT, Japan.

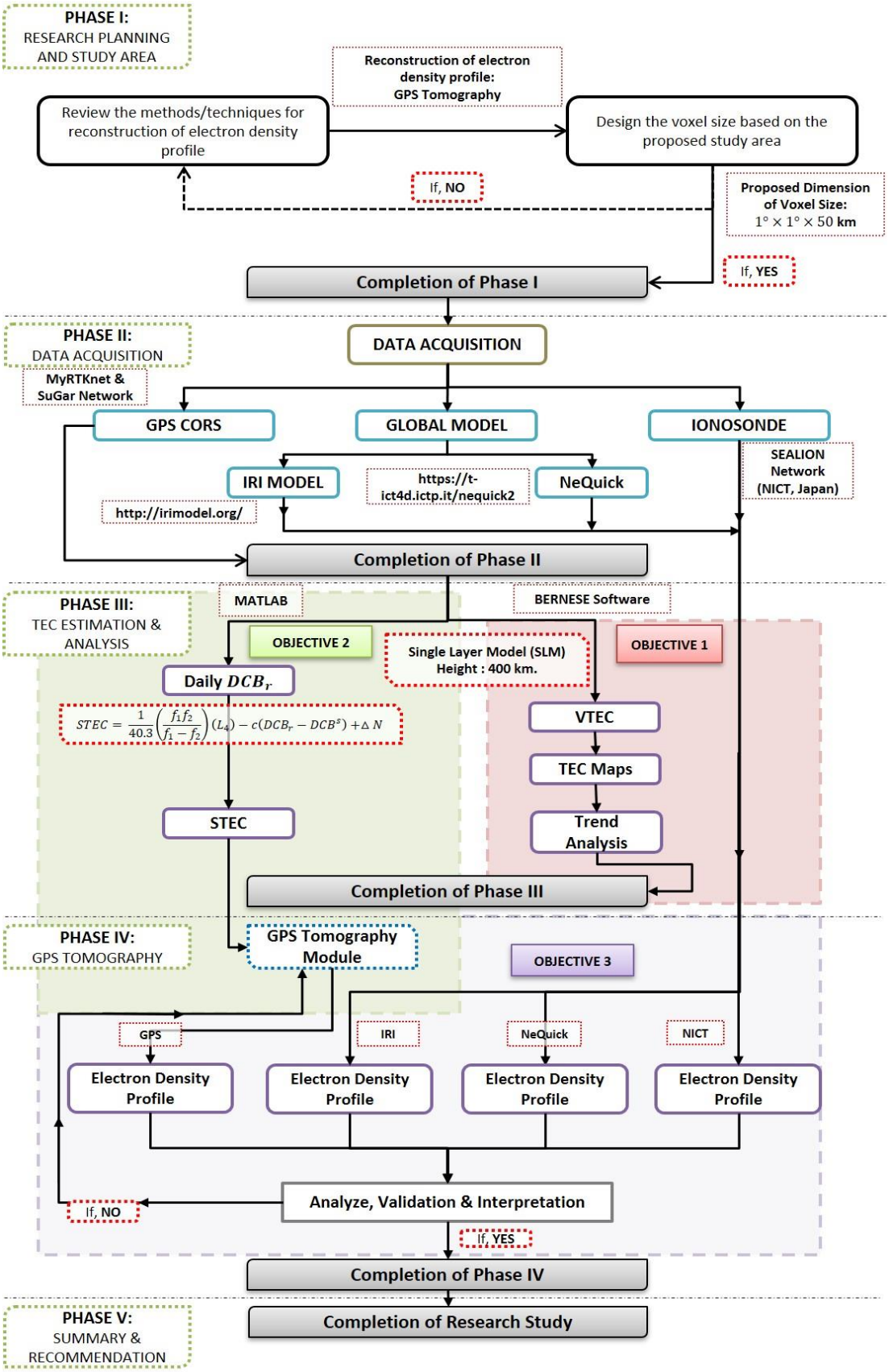

Figure 1.3 The schematic flow of the study.

PHASE III: TEC Estimation and Analysis

1. In this phase, the TEC has been estimated by using Bernese software version 5.0 for TEC trend analysis. The precise point positioning module has been used, where this module adopted the SLM mapping function. In this study, the height of the maximum densities of electron is assumed about 400 km (Leong *et al*, 2009*)*.

2. For GPS tomography module, the estimation of STEC has been computed using Matlab software (refer Appendix D). This estimation process takes into consideration of the design voxel for study area that has been proposed in Phase I.

PHASE IV: GPS Tomography

1. In this phase, the STEC that has been estimated from Phase III and secondary data from Phase II have been used as input for the tomography.

2. The electron density profile has been reconstructed in this phase by adopting the tomography technique. The global ionospheric model has been retrieved and used as a background model during the reconstruction.

3. The validation of the reconstruction from GPS ionospheric tomography has been carried out with the global model and ionosonde measurements trend analysis of the tomography has been discussed briefly in this phase.

PHASE V: Summary and Recommendation

All the procedure, results and assessment have been summarized in this phase. The recommendation and improvement for modelling the electron density profile over Malaysia has been suggested in this phase.

1.7 Thesis Structure and Organization

The thesis outline was carefully organized to clearly show the research flow from the first chapter to the seventh chapter.

Chapter 1: Introduction

This chapter gives an overview of the background of the study, identifying the problem statements and the objectives to overcome those issues. This chapter also contains the significance of this study to highlight the importance of this study towards current infrastructure.

Chapter 2: Literature Review

This chapter review on the morphology of the ionosphere over the Malaysian region, where the GPS TEC mapping and its trend over the study area. The TEC maps are presented in 2D maps and discussed based on its temporal, diurnal, spatial and month-to-month variations. A thorough and critical reviews in limitation 2D TEC maps presents the ideas and concepts to this current study.

Chapter 3: Methodology I: Estimation of Receiver Code Bias

This chapter present a method to obtain a reliable method in estimation of receiver code bias in support the development of the tomography module. This chapter also explains the method of the calculation and analysis of the receiver code bias that will be used in this study.

Chapter 4: Methodology II: Reconstruction of Ionospheric Profile using Tomography technique

This chapter discussed on a method to reconstruct the 3D ionospheric profiles over the study area. This reconstruction has been proposed to overcome the limitation of the 2D TEC maps as well as to achieve the aim of this study. This method has been reviewed, and its theories and concept has been discussed briefly in this chapter.

Chapter 5: Result and Analysis

Chapter 5 presented the result and analysis with the discussion. The assessment of the GPS ionospheric tomography with the global ionospheric models and ionosonde measurements has been carried out during the quiet and disturbed conditions of the ionosphere. At the end of this chapter, the analysis of the assessment will be presented.

Chapter 6: Case Study: Detection of Equatorial Plasma Bubble using Tomography

This chapter presents the tomography methods to detect the signature of equatorial plasma bubbles (EPB), one of the ionospheric irregularities that occurred over the equatorial region. In doing so, two (2) previous studies has been used as a reference to detect the signature of EPB. The results and analysis of the detection of EPB signatures has been presented at the end of the chapter.

Chapter 7: Conclusion and Recommendation

Lastly, this chapter contains summary of the main findings of this study as well as the recommendation that can be used to support the space weather studies and continuous ionospheric monitoring in the study area.

REFERENCES

Abadi, P., Otsuka, Y. and Tsugawa, T. (2015). Effects of pre-reversal enhancement of ExB drift on the latitudinal extension of plasma bubble in Southeast Asia. *Earth, Planets and Space, 67*(1), 74.

Abid, M.A., Mousa, A., Rabah, M. and Awad, A. (2016). Temporal and spatial variation of differential code biases: A case study of regional network in Egypt. *Alexandria Engineering Journal, 55*(2). 1507-1514.

Abdu, M.A. (2005) Equatorial ionosphere thermosphere system: electrodynamics and irregularities. *Advances in Space Research, 35*(5), 771-787.

Abdu, M.A. (2016) Electrodynamics of ionospheric weather over low latitudes. *Geoscience Letters, 3* (1), 11.

Aggarwal, M. (2011). TEC variability near northern EIA crest and comparison with IRI model. *Advances in Space Research, 48* (7). 1221-1231.

Arikan, F., Nayir, H., Sezen, U. and Arikan, O. (2008). Estimation of single station interfrequency receiver bias using GPS-TEC. *Radio Science,43* (4).

Austen, J.R., Franke, S.J., Liu, C.H. and Yeh, K.C. (1986). Application of computerized tomography techniques to ionospheric research. In *International beacon satellite symposium on radio beacon contribution to the study of ionization and dynamics of the ionosphere and to corrections to geodesy and technical workshop.* 22-35.

Baba, M.A. (2016) Assessment of CODE-GIM and Local Derived Total Electron Content (TEC). B. Sc. Thesis. Universiti Teknologi Malaysia.

Bagiya, M.S., Joshi, H.P., Iyer, K.N., Aggarwal, M., Ravindran, S. and Pathan, B.M. (2009). TEC variations during low solar activity period (2005-2007) near the Equatorial Ionospheric Anomaly Crest region in India. *Annales Geophysicae, 27.*1047-1057. Bahari, S.A., Abdullah, M. and Hasbi, A.M. (2015). A Review of Ionospheric Studies in Malaysia using GPS. In *Space Science and Communication (IconSpace), 2015 International Conference on.* IEEE.

Belehaki, A., Kutiev, I., Tsagouri, I. and Marinov, P. (2015). Characteristics of large scale travelling ionospheric disturbances exploiting ground-based ionograms, GPS-TEC and 3D electron density distribution maps. In *Proceeding 14th*

International Ionospheric Effects Symposium (IES-2015), Alexanderia, Virginia. 12-14.

Bender, M., Dick, G., Ge, M., Deng, Z., Wickert, J. Kahle, H., Raabe, A. and Tetzlaff, G. (2011). Development of GNSS water vapour tomography system using algebraic reconstruction techniques. *Advances in Space Research, 47* (10). 1704-1720.

Bilitza, D. (2001). International Reference Ionosphere 2000. *Radio Science,36*(2). 261-275.

Bilitza, D., McKinnell, L.A., Reinisch, B. and Fuller-Rowell, T. (2011). The international reference ionosphere today and in the future. *Journal of Geodesy, 85*(12).909-920.

Buhari, S.M., Abdullah, M., Hasbi, A.M., Otsuka, Y., Yokoyama, T., Nishioka, M. and Tsugawa, T. (2014). Continuos generation and two-dimensional structure of equatorial plasma bubbles observed by high-density GPS receivers in Southeast Asia. *Journal of Geophysical Research: Space Physics,119*(12). 10-569.

Buhari, S.M., Abdullah, M., Yokoyama, T., Hasbi, A.M., Otsuka, Y., Nishioka, M., Bahari, S.A. and Tsugawa, T. (2015). Climatology of Equatorial Plasma Bubble Observed by MyRTKnet over the Years 2008-2013. *Space Science and Communication (IconSpace), 2015 International Conference IEEE.* 101-105.

Bust, G.S., Garner, T.W. and Gaussiran, T.L. (2004). Ionospheric Data Assimilation Three-Dimensional (IDA3D): A global multisensory, electron density specification algorithm. *Journal of Geophysical Research: Space Physics, 109*(A11).

Chakraborty, S.K. and Hajra, R. (2009). Electrojet control of ambient ionization near the crest of the equatorial anomaly in the Indian zone. In *Annales Geophysicae: Atmospheres, hydrospheres and space sciences, 27*(1). 93-105.

Chapagain, N.P., Fisher, D.J., Meriwether, J.W., Chau, J.L. and Makela, J.J. (2013). Comparison of zonal neutral winds with equatorial plasma bubble and plasma drift velocities. *Journal of Geophysical Research: Space Physics, 118*(4), 1802-1812.

Chapagain, N.P., Taylor, M.J., and Eccles, J.V. (2011). Airglow observations and modeling of F region depletion zonal velocities over Christmas Island. *Journal Geophysical Research: Space Physics, 116*(A2).

Chen, C.H., Saito, A., Lin, C.H., Yamamoto, M., Suzuki, S. and Seemala, G.K. (2016). Medium-scale travelling ionospheric disturbances by three-dimensional ionospheric GPS tomography. *Earth, Planets and Space, 68*(1).32.

Chen, W., Hu, C., Gao, S., Chen, Y., Ding, X. and Simon, C.W.K. (2004). Absolute ionospheric delay estimation based on GPS PPP and GPS active network. In *International Symposium on GNSS/GPS, Sydney, Australia.*

Chiablaem, A., Phakphisut, W., and Supnithi, P. (2017). Study of GPS instrumental bias and TEC estimations from GPS stations in Thailand. In *14th International Conference Electrical Engineering/Electronics, Computer, Telecommunications and Information Technology (ECTI-CON).* 810-813. IEEE.

Choi, B.K., Cho, J.H. and Lee, S.J. (2011). Estimation and analysis of GPS receiver differential code biases using KGN in Korean Peninsula. *Advances in Space Research, 47* (9). 1590-1599.

Choi, B.K., Chung, J.K. and Cho, J.H. (2010). Receiver DCB estimation and analysis by types of GPS receiver. *Journal of Astronomy and Space Science, 27.* 123-128.

Choi, B.K., Park, J.U. & Chung, J.K. (2006). Ionospheric Tomography using A Regional GPS Network over South Korea. *Positioning,1*(10).47-51.

Chung, J.K., Yoo, S.M. and Lee, W. (2016). The First Measurement of Seasonal Trends in the Equatorial Ionospheric Anomaly trough at the CHUK GNSS Site During the Solar Maximum in 2014. *Journal of Astronomy and Space Sciences, 33*(4). 287-293.

Comberiate, J.M., Kamalabadi, F. and Paxton, L. (2006). Tomographic imaging of equatorial plasma bubbles. *Geophysical Research Letters, 33*(15).

Dach, R and Walser, P. (2013). Bernese GNSS Software Version 5.0.

Das, S.K. abd Shukla, A.K. (2011). Two-dimensional ionospheric tomography over the low-latitude Indian region: An intercomparison of ART and MART algorithm. *Radio Science, 46*(2). 1-13.

Dear, R.M. and Mitchell, C.N. (2006). GPS interfrequency biases and total electron content errors in ionospheric imaging over Europe. *Radio Science, 41*(6).

Debao, W. and Yiyan, Z. (2011). Application of ionospheric tomography inversion to GPS data to study ionospheric electron density distribution over China. *Geodesy*

Dubey, S., Wahi, R. and Gwal, A.K. (2006). Ionospheric effects on GPS positioning. *Advances in Space Research, 38*(11), 2478-2484.

Encyclopedia Britannica, Retrieved from https://www.britannica.com/

Frey, H.U., Frey, S., Larson, D., Nygren, T. and Semeter, J. (1998). Tomographic methods for magnetospheric applications. *Science closure and enabling technologies for constellation class missions*. 72-77.

Fukao, S., Yokoyama, T., Tayama, T., Yamamoto, M., Maruyama, T. and Saito, S. (2006). Eastward traverse of equatorial plasma plumes observed with the Equatorial Atmosphere Radar in Indonesia. In *Annales Geophysicae* (Vol. 24, No. 5, 1411-1418). Copernicus GmbH.

Garcia, R. and Crespon, F. (2008). Radio tomography of the ionosphere: Analysis of and underdetermined, ill-posed inverse problem and regional application. *Radio Science, 43*(2).

Global Ionosphere Radio Observatory (GIRO). Retrieved on 23rd September 2017 via http://giro.uml.edu .

Hernandez-Pajares, M., Juan, J.M., Sanz, J. and Bilitza, D. (2002). Combining GPS measurements and IRI model values for space weather specification. *Advances in Space Research, 29*(6). 949-958.

Hocke, K. and Igarashi, K. (2002). Structure of the earth's lower ionosphere observed by GPS/MET radio occultation. *Journal of Geophysicae Research, 107*(A5).

Hoffman-Wellenhof, B., Lichtenegger, H. and Wasle, E. (2007). *GNSS-Global Navigation Satellite Systems GPS, GLONASS, Galileo, and more*. Springer Science and Business Media.

Hong, C.K., Grejner-Brzezinska, D.A and Kwon, J.H. (2008). Efficient GPS receiver DCB estimation for ionosphere modeling using satellite-receiver geometry changes. *Earth Planers Space, 60*(11). E25-e28.

Hong, J., Kim, Y.H., Chung, J.K., Ssessanga, N. and Kwak, Y.S. (2017). Tomography Reconstruction of Ionospheric Electron Density with Empirical Orthonormal Functions Using Korea GNSS Network. *Journal of Astronomy and Space Sciences, 34*(1), 7-17.

Huang, C.S., de La Beaujardiere, O., Roddy, P.A., Hunton, D.E., Ballenthin, J.O. and Hairston., M.R. (2012). Generation and characteristics of equatorial plasma bubbles detected by the C/NOFS satellite near the sunset terminator. *Journal of Geophysical Research: Space Physics, 117*(A11).

Immel, T.J., Sagawa, E., England, S.L., Henderson, S.B., Hagan, M.E., Mende, S.B., Frey, H.U., Swenson, C.M. and Paxton, L.J. (2006). Control of equatorial ionospheric morphology by atmospheric tides. *Geophysical Research Letters, 33*(15).

International GNSS Service (IGS). Retrieved from http://www.igs.org.

International Reference Ionosphere (IRI), Retrieved from http://irimodel.org.

Jin, R., Jin, S. and Feng, S. (2012). M_DCB: Matlab code for estimating GNSS satellite and receiver differential code biases. *GPS Solutions, 16*(4). 541-548.

Jin, S. and Jin, R. (2011). GPS Ionospheric Mapping and Tomography: A Case of Study in a Geomagnetic Storm. In *Geoscience and Remote Sensing Symposium (IGARSS), 2011 IEEE International*. 1127-1130. IEEE.

Jin, S. and Park, J.U. (2007). GPS Ionospheric tomography: A comparison with the IRI-2001 model over South Korea. *Earth, Planets and Space, 59*(4). 287-292.

Jin, S., Luo, O.F. and Park, P. (2008). GPS observations of the ionospheric F2-layer behavior during the 20th November 2003 geomagnetic storm over South Korea. *Journal of Geodesy, 82*(12). 883-892.

Jin, S., Park, J.U., Wang, J.L., Choi, B.K. and Park, P.H. (2006). Electron Density Profiles Derived from Ground-Based GPS Observations. *The Journal of Navigation, 59*(3). 395-401.

Kao, S.P., Chen, Y.C. and Ning, F.S. (2014). A MARS-based method for estimating regional 2-D ionospheric VTEC and receiver differential code bias. *Advances in Space Research, 53*(2). 190-200.

Kassa, T., Damtie, B., Bires, A., Yizengaw, E. and Ciliers, P. (2015). Spatio-temporal characteristics of the Equatorial Ionization Anomaly (EIA) in the East African region via ionospheric tomography during the year 2012. *Advances in Space Research, 55*(1), 184-198.

Kee, C. and Yun, D. (2002). Extending coverage of DGPS by considering atmospheric models and corrections. *The Journal of Navigation, 55*(2). 305-322.

Keshin, M. (2012) A new algorithm for single receiver DCB estimation using IGS TEC maps. *GPS Solutions, 16*(3). 283-292.

Khamdan, S.S., Musa, T.A., Wijaya, D.D. and Buhari, S.M. (2018). The estimation of receiver code bias for MyRTKnet stations. In *IOP Conference Series: Earth and Environmental Science, 169(*1). IOP Publishing.

Kil, H. (2015). The Morphology of Equatorial Plasma Bubbles – a review. *Journal of Astronomy and Space Science, 32*(1). 13-19.

Kintner, P. M., B. M. Ledvina, and E. R. de Paula (2007). GPS and ionospheric scintillations. *Space Weather, 5*(9).

Kong, J. Yao, Y., Liu, L, Zhai, C. and Wang, Z. (2016). A new computerized ionosphere tomography model using the mapping function and an application to the study of seismic ionosphere disturbance. *Journal of Geodesy, 90* (8), 741-755.

Lee, J.K., Kamalabadi, F. and Makela, J.J. (2008). Three-dimensional tomography of ionospheric variability using a dense GPS receiver array. *Radio Science, 43*(3).

Leong, S. K., Musa, T. A., Abdullah, K. A., Othman, R., Lim, S., Rizos, C. (2009). GPS-Derived Local TEC Mapping over Peninsula Malaysia during Solar Minimum of Sunspot Cycle 24. In *Proceedings of the South East Asian Survey Congress (SEASC) 2009*.

Leong, S.K. (2013). Network-based Real-time Kinematic Ionospheric Residual Modelling and Integrity Monitoring System. Master Thesis. Universiti Teknologi Malaysia.

Leong, S.K., Musa, T.A., Omar, K., Subari, M.D., Pathy, N.B. and Asilam, M.F. (2015). Assessment of ionosphere models at Banting: Performance of IRI-2007, IRI-2012 and NeQuick 2 models during the ascending phase of Solar Cycle 24. *Advances in Space Research, 55*(8). 1928-1940.

Liu, J., Chen, R., Wang, Z. and Zhang, H. (2011). Spherical cap harmonic model for mapping and predicting regional TEC. *GPS solutions, 15*(2), 109-119.

Liu, L., He, M., Yue, X., Ning, B. and Wan, W. (2010). Ionosphere around equinoxes during low solar activity. *Journal of Geophysical Research: Space Physics, 115*(A9).

Liu, L., Wan, W., Ning, B., Pirog, O.M. and Kurkin, V.I. (2006). Solar activity variations of the ionospheric peak electron density. *Journal of Geophysical Research: Space Physics, 111*(A8).

Liu, Z.Z. and Gao, Y. (2001). Ionospheric Tomography Using GPS Measurements. In Proceedings of the International Symposium on Kinematic Systems in Geodesy, Geomatics & Navigation. 111-120.

Lu, W. and Yin, F.F. (2004) Adaptive algebraic reconstruction technique: Adaptive algebraic reconstruction technique. *Medical Physics, 31* (12). 3222-3230.

Luhr, H. and Xiong, C. (2010). IRI-2007 model overestimates electron density during the 23/24 solar minimum. *Geophysical Research Letters, 37*(23).

Ma, G. and Maruyama, T. (2003) Derivation of TEC and estimation of instrumental biases from GEONET in Japan. *Annales Geophysicae, 21*(10). 2083-2093.

Magdaleno, S., Herraiz, M., Altadil, D, and de la Morena, B. (2017). Climatology characterization of equatorial plasma bubbles using GPS data. *Journal of Space Weather and Space Climate, 7*(A3).

McCaffrey, A.M., Jayachandran, P.T., Themens, D.R. and Langley, R.B. (2017). GPS receiver CODE bias estimation: A comparison of two methods. *Advances in Space Research, 59*(8), 1984-1991.

Minkwitz, D., van den Boogaart, K.G., Gerzen, T. and Hoque, M. (2015). Tomography of the ionospheric electron density with geostatistical inversion. In *Annales Geophysicae, 33*(8). 1071-1079

Muella, M.T.A.H., de Paula, E.R., Mitchell, C.N., Kitner, P.M. Paes, R.R. and Batista, I.S. (2011). Tomographic imaging of the equatorial and low-latitude ionosphere over central-eastern Brazil. *Earth Planets Space, 63*(2). 129-138.

Musa, T.A., Leong, S.K., Abdullah, K.A. and Othman, R. (2012). ISKANDARnet IOMOS: Near real-time equatorial space weather monitoring and alert system in Peninsular Malaysia. *Space Weather, 10*(11). 1-15.

National Institute of Information and Communications Technology (NICT). Retrieved from https://www.nict.go.jp/en/

National Oceanic and Atmospheric Administration (NOAA). (2018). Flare Index of Solar Activity. Retrieved January 20, 2018, from https://www.ngdc.noaa.gov/

Nayir, H., Arikan, F., Arikan, O. and Erol, C.B. (2007). Total electron content estimation with Reg-Est. *Journal of Geophysical Research: Space Physics, 112*(A11).

NeQuick Model. Retrieved from https://t-ict4d.ictp.it/nequick-2-web-model.

Niranjan, K., Srivani, B., Gopikrishna, S. and Rama Rao, P.V.S. (2007). Spatial distribution of ionization in the equatorial and low-latitude ionosphere of the Indian sector and its effect on the Pierce point altitude for GPS application during low solar activity periods. *Journal of Geophysicae, 112*(A05304).

Nishioka, M., Saito, A. and Tsugawa, T. (2008). Occurrence characteristics of plasma bubble derived from global ground-based GPS receiver networks. *Journal of Geophysical Research: Space Physics, 113* (A5).

Okoh, D., McKinnel, L.A., Cilliers, P., Okere, B., Okonkwo, C. and Rabiu, B. (2015). IRI-vTEC versus GPS-vTEC for Nigerian SCINDA GPS stations. *Advances in Space Research, 55*(8). 1941-1947.

OMNIWeb Nasa https://omniweb.gsfc.nasa.gov

Oryema, B., Jurua, E. and Ssebiyonga, N. (2016). Variations of Crest-to-Trough TEC ratio of the East African Equatorial Anomaly Region. *International Journal of Astrophysics and Space Science. 4*(1). 12-20.

Otsuka, Y., Ogawa, T., Saito, A., Tsugawa, T., Fukao, S. and Miyazaki, S. (2002). A new technique for mapping of total electron content using GPS network in Japan. *Earth, Planets and Space, 54*(1). 63-70.

Otsuka, Y., Shiokawa, K., Ogawa, T., Yokoyama, T., Yamamoto, M. and Fukao, S. (2004). Spatial relationship of equatorial plasma bubbles and field-alligned irregularities observed with an all-sky airglow imager and the Equatorial Atmosphere Radar. *Geophysical Research Letter, 31*(20).

Radzi, Z.M., Abdullah, M., Hasbi, A.M., Mandeep, J.S. and Bahari, S.A. (2013). Seasonal variation of Total Electron Content at equatorial station, Langkawi, Malaysia. In *Space Science and Communication (IconSpace), 2013 IEEE International Conference on,*186-189.IEEE.

Ray, S., Paul, A. and Dasgupta, A. (2006). Equatorial scintillations in relation to the development of ionization anomaly. In *Annales Geophysicae, 24*(5). 1429-1442.

Saito, S., Suzuki, S., Yamamoto, M., Saito, A. and Chen, C.H. (2017). Real-Time Ionosphere Monitoring by Three-Dimensional Tomography over Japan. *Navigation: Journal of the Institute of Navigation, 64* (4), 495-504.

Sarudin, I., Hamid, N.S.A., Abdullah, M and Buhari, S.M. (2017). Investigation of zonal velocity of equatorial plasma bubbles (EPBs) by using GPS data. In *Journal of Physics: Conference Series, 852*(1). IOP Publishing.

Seemala, G.K., Yamamoto, M., Saito, A. and Chen, C.H. (2014). Three-dimensional GPS ionospheric tomography over Japan using constrained least squares. *Journal of Geophysical Research: Space Physics, 119*(4). 3044-3052.

Shiokawa, K., Otsuka, Y. Ogawa, T. and Wilkinson, P. (2004). Time evolution of high-altitude plasma bubbles imaged at geomagnetic conjugate points. *Annales Geophysicae, 22*(9). 3137-3143.

Sibanda, P. and McKinnell, A. (2011). Topside ionospheric vertical electron density profile reconstruction using GPS and ionosonde data: possibilities for South Africa. In *Annales Geophysicae, 29*(2).

Space Weather Prediction Center (SWPC), Retrieved from http://www.swpc.noaa.gov.

Stolle, C., Schluter, S., Jacobi, C. and Jakowsli, N. (2003). 3-dimensional ionospheric electron density reconstruction based on GPS measurements. *Advances in Space Research, 31*(8). 1965-1970.

Ssessanga, N., Kim, Y.H. and Kim, E. (2015). Vertical structure of medium-scale travelling ionospheric disturbances. *Geophysical Research Letter, 42*(21). 9156-9165.

Sunehra, D. (2013). Validation of GPS receiver instrumental bias results for precise navigation. *Indian Journal of Radio & Space Physics, 42.*175-181.

Tan, L.M., Shiokawa, K., Thu, N.N., and Ha, T.Q. (2017). Electron density variability of nighttime D region ionosphere in Vietnamese and Japanese sectors. *Journal of Geophysical Research: Space Physics, 122*(6). 6543-6551.

Tan, L.M., Thu, N.N., Ha, T.Q. and Luong, Q.N. (2015). Seasonal variations of nighttime D-region ionosphere in 2013 solar maximum observed from a low-latitude station. *Earth, Planets and Space.*

Tang, J., Yao, Y., Kong, J. and Zhang, L. (2016). Large-scale travelling ionospheric disturbances using ionospheric imaging at storm time: A case study on 17 March 2013. *Journal of Atmospheric and Solar-Terrestrial Physics, 145.*12-20.

Tariku, Y.A. (2015). TEC prediction performance of IRI-2012 model during a very low and a high solar activity phase over equatorial region, Uganda. *Journal of Geophysical Research: Space Physics, 120*(7), 5973-5982.

Thampi, S.V., Pant, T.K., RAvindran, S., Devasia, C.V. and Sridharan, R. (2004). Simulation studies on the tomographic reconstruction of the equatorial and low-latitude ionosphere in the context of the Indian tomography experiment: CRABEX. In *Annales Geophysicae, 22*(10). 3445-3460.

Thampi, S.V., Ravindran, S., Devasia, C.V., Sreelatha, P., Pant, T.K., Sridharan, R., Ratnam, Sarma, A.D., Reddi, C.R., Jose, J. and Sastri, J.H. (2007) Coherent Radio Beacon Experiment (CRABEX) for tomographic imaging of the

equatorial ionosphere in the Indian longitudes – Preliminary results. *Advances in Space Research, 40*93), 436-441.

Tsugawa, T., Nishioka, M., Ishii, M., Hozumi, K., saito, S., Shinbori, A., Otsuka, Y., Saito., A., Buhari, S.M., Abdullah, M. and Supnithi, P. (2018). Total electron content observations by dense regional and worldwide International Networks of GNSS. *Journal of Disaster Research, 13*(3), 535.

Tsunoda, R.T. (2010). On equatorial spread F: Establishing a seeding hypothesis. *Journal of Geophysical Research, 115*(A12).

Tsunoda, R.T. (2015). Upwelling: a unit of disturbance in equatorial spread F. *Progress in Earth and Planetary Science, 2*(1). 9.

Van de Kamp, M.M.J.L. (2013). Medium-scale 4-D ionospheric tomography using a dense GPS network. In *Annales Geophysicae, 31*(1). 75.

Wen, D., Yuan, Y. and Ou, J. (2007). Monitoring the three-dimensional ionospheric electron density distribution using GPS observations over China. *Journal of earth system science, 116*(3). 235-244.

World Data Geomagnetism, Kyoto. Retrieved on 15 June 2018, from http://wdc.kugi.kyoto-u.ac.jp/cgi-bin/kp-cgi

Ya'acob, N., Abdullah, M. and Ismail, M. (2010). GPS Total Electron Content (TEC) prediction at ionosphere layer over the equatorial region. In *Trends in Telecommunications Technologies.* InTech.

Yigit, E., Frey, H.U., Moldwin, M.B., Immel, T.J. and Ridley, A.J. (2016). Hemispheric differences in the response of the upper atmosphere to the august 2011 geomagnetic storm: A simulation study. *Journal of Atmospheric and Solar-Terrestrial Physics, 141*, 13-26

Yokoyama, T., Fukao, S. and Yamamoto, M. (2004). Relationship of the onset of equatorial F region irregularities with the sunset terminator observed with the Equatorial Atmosphere Radar. *Geophysical Research Letters, 31*(24).

Zhang, B., Teunissen, P.J., Yuan, Y., Zhang, H. and Li, M. (2017). Joint estimation of vertical total electron content (VTEC) and satellite differential code biases (SDCBs) using low-cost receivers. *Journal of Geoodesy.* 1-13.

Zhang, D.H., Zhang, W., Li, Q., Shi, Q.L., Hao, Y.Q. and Xiao, Z. (2010) Accuracy analysis of the GPS instrumental bias estimated from observations in middle and low latitudes. *Annales Geophysicae, 28*(8), 1571-1580.

Zhou, K., Li, Z., Yuan, H. and Wang, L. (2015). Three dimensional ionospheric model using Global GNSS Network data. *Journal of IPNT, 1*(1), 1-8.

Zolesi, B. and Cander, L.R. (2014). *Ionospheric prediction and forecasting.* Springer Berlin Heidelberg.

.